PROJECT 2

Resting state analysis before and after exoskeleton-assisted gait

1. Introduction

Neurorehabilitation is the process aimed to compensate for motor or cognitive deficits. This clinical practice is based on neuroplasticity, which can be defined as the ability of the central nervous system to reorganize its structures, functions, and connections in response to life experience. Nowadays, the traditional approach to rehabilitation has been renewed by the development of cutting-edge technologies. For instance, exoskeletons are robotic devices used for neurorehabilitation to help patients affected by motor disabilities, such as gait impairment. Exoskeleton-Assisted Gait (EAG) training could facilitate early mobilization in subjects who are unable to maintain the upright position by providing repetitive, high-intensity, and high-dose practices compared to traditional rehabilitation [1]. Furthermore, the use of an exoskeleton allows to reduce the physical effort required from the therapists during traditional rehabilitative sessions, which involve at least three experts to support manually the legs and torso of the patient to perform the training [2].

One way to assess the effects of EAG could be to analyse the electroencephalographic (EEG) signal. Past studies showed that brain activity exhibits a fractal nature [3], which means that it has a temporal organization over multiple time scales. For this reason, nonlinear approaches based on fractal metrics, such as the Higuchi's fractal dimension (FD), could lead to relevant insights. Particularly, the fractal nature of a signal has often been exploited to quantify the topological and functional complexity of processes generating that signal [3]: FD value decreases dramatically during very regular electrical activity [4]. Nonlinear complexity indicators based on fractal analysis are particularly suitable for real-time applications, having lower computational cost than other nonlinear entropy-based metrics.

Scarpa et al. in [5] and Rubega et al. in [6] demonstrated that EEG signal recorded during hypoglycemia is characterized by a decrease in Higuchi's FD compared with EEG signal recorded during euglycemia, highlighting that an EEG signal tends to be less complex during hypoglycemia. Rubega et al. in [7] showed that Higuchi's index can be used for a better tailoring of rehabilitation processes after a stroke: its values were significantly lower after the very early stage following a stroke, reflecting a significantly less complex brain activity than healthy controls.

In this project, we investigated EEG variations induced by a single session of EAG through both a linear approach, based on the relative power spectra in the canonical EEG frequency bands, and a nonlinear method, based on Higuchi's FD, being them possible biomarkers to assess the effectiveness of EAG.

2. Materials and methods

2.1 Database

The dataset is composed of EEG data coming from a single healthy person and acquired using a 64-channels system, in a resting state condition with eyes open at two time points: before and after a single session of EAG. Thus, we dealt with two signals: the one acquired before the task (pre-signal) and the one acquired after the EAG (post-signal). The sampling rate is 250 Hz.

2.2 Pre-processing

The data were processed in Matlab R2022 using personalized scripts based on EEGLAB toolbox. We apply the same pre-processing steps, in sequence, to the pre-signal and to the post-signal. The two recordings were band-pass filtered between 1 and 30 Hz as shown in Figure 1. We interpolated two bad channels, previously selected in two ways: one considering the mean of the standard deviation of the signal (Figure 2) and the second by visual inspecting the signal's scroll plot.

```
8      %% PRE
9 -    load('resting_pre.mat')
10 -   data_pre = EEG_import';
11
12 -   fs = 250; %[Hz]
13 -   T = 1/fs; %[s]
14 -   Ns = size(data_pre,1);
15 -   Nch = size(data_pre,2);
16
17     % filtering
18     % high pass at 1Hz
19 -   fc = 1; %Hz
20 -   [b,a] = butter(4, fc/(fs/2), 'high') ;
21 -   data_pre_filt = filtfilt(b,a,data_pre);
22
23     % low pass at 30Hz
24 -   fc = 30; %[Hz]
25 -   [b,a] = butter(4, fc/(fs/2), 'low') ;
26 -   data_pre_filt = filtfilt(b,a,data_pre_filt);
```

Figure 1: Matlab code used for the 1 to 30 Hz filtering of the pre-signal. A similar code was implemented for the filtering of the post-signal.

```
28     % selecting bad channels considering SD
29 -   averageSD = mean(std(data_pre_filt));
30 -   badCh = std(data_pre_filt) > 3*averageSD;
31
32 -   if ~any(badCh)
33 -       disp("there aren't bad channels")
34 -   else
35 -       chToInterpolate = find(badCh);
36 -       disp(['bad channels to be interpolated: ', num2str(chToInterpolate)])
37 -   end
38
```

Figure 2: Matlab code used for the selection of bad channels considering the mean of the standard deviation of the pre-signal. A similar code was implemented for the filtering of the post-signal.

Eye movements, cardiac activity, muscle activity and line noise were removed from the EEG signal using the independent component analysis (FastICA algorithm) based on the waveform, topography, time-course, and the activity power spectrum of the component. Figure 3, 4, 5, 6 show four examples of rejected components.

Finally, data were re-referenced to the average reference.

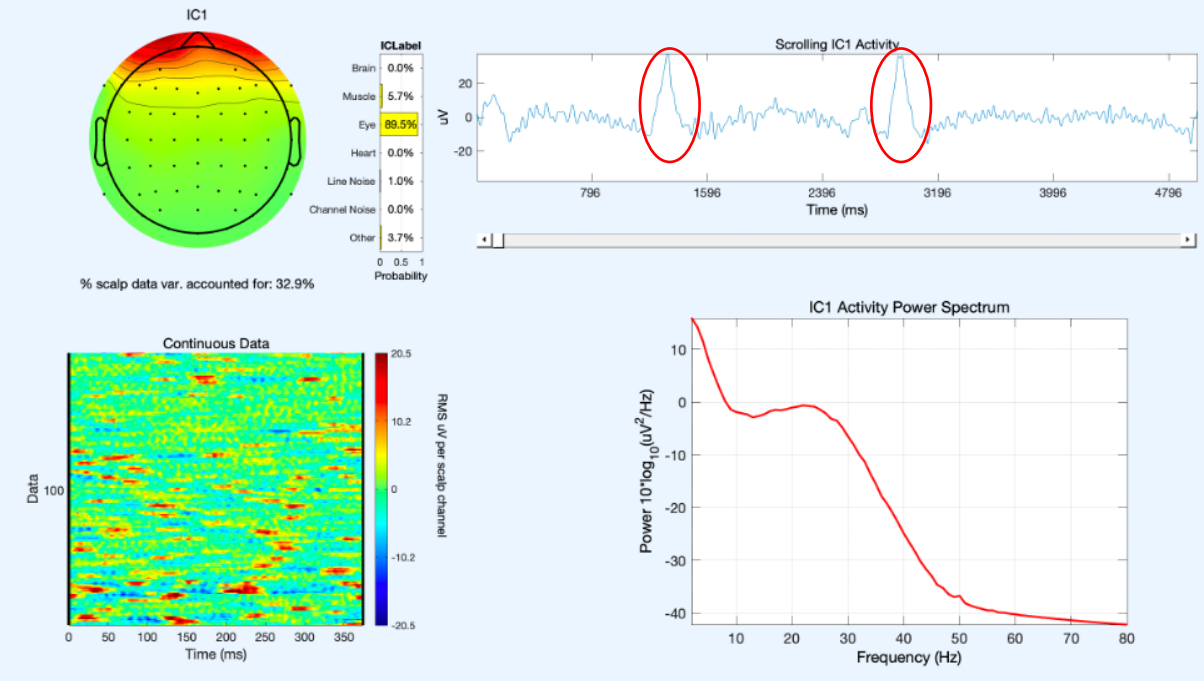

Figure 3: Example of component rejected because containing information about eye movement. The top-right and the bottom-left plots shows the typical peaks (red circles) due to the blink of the eye.

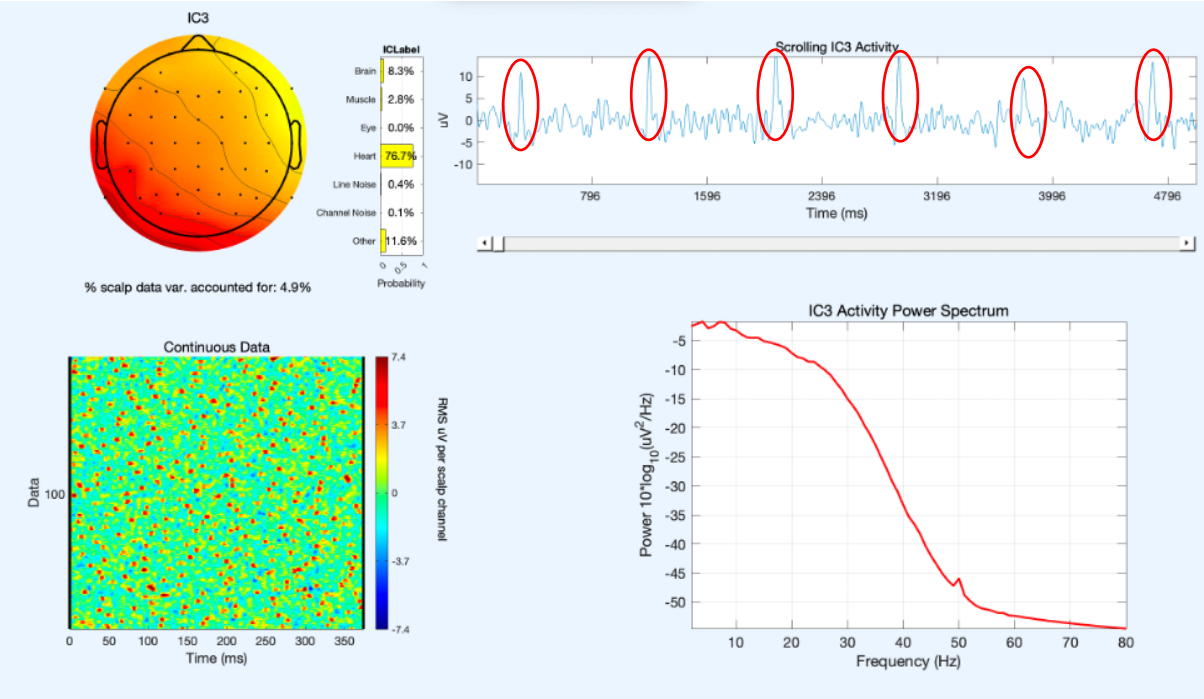

Figure 4: Example of component rejected because containing information about the cardiac activity. The top-right and the bottom-left plots shows peaks (red circles) probably generated by the heartbeat. Furthermore, the topoplot shows the typical diagonal distribution.

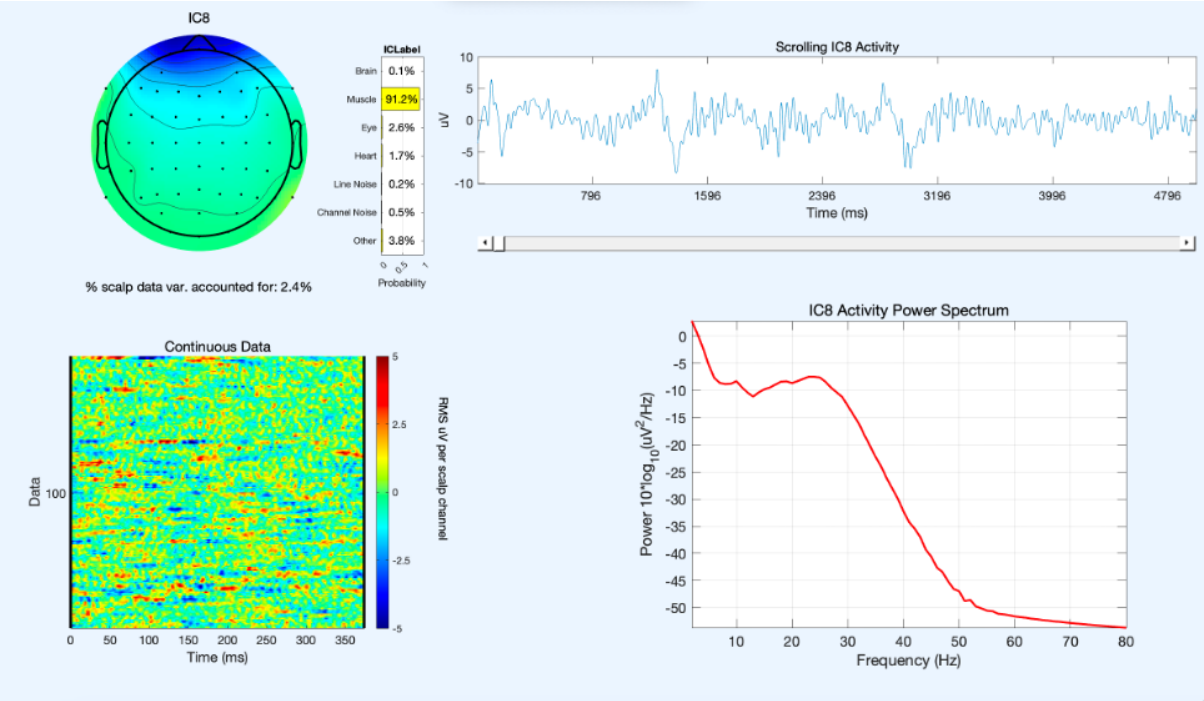

Figure 5: Example of component rejected because containing information about muscle activity. The bottom-left plot shows the typical "cheetah spots" distribution.

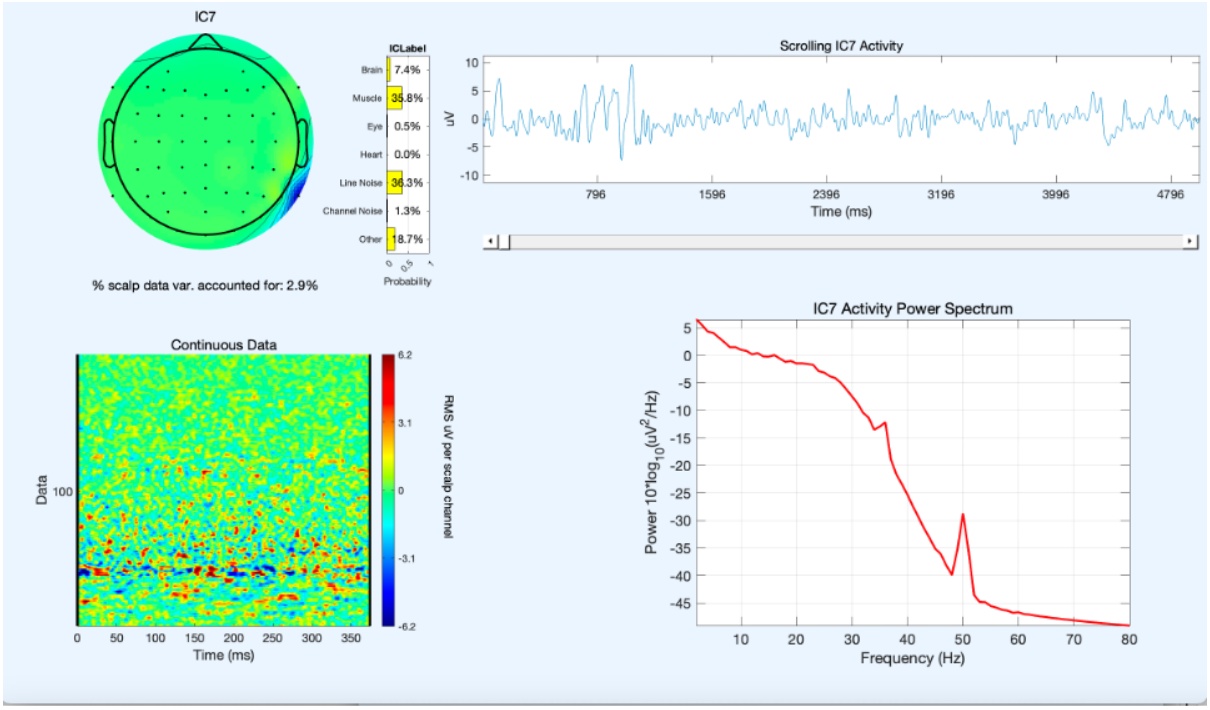

Figure 6: Example of component rejected because containing line noise. The bottom-right plot shows a peak at 50 Hz.

2.3 Linear Analysis - Power spectra

During the linear analysis, the average spectrum was calculated using Welch's overlapped segment averaging estimator (pwelch function in Matlab). The relative power spectra in the canonical EEG frequency bands were estimated for each channel by dividing the average power of each frequency

band ([1-4] Hz for delta band, [4-8] Hz for theta band, [8-13] Hz for alpha band and [13-30] Hz for beta band) with the total power in the range [1-30] Hz.

2.4 Non-Linear Analysis - Fractal Dimension Measure

The fractal dimension (FD) provides a complexity index that describes how the measure of the length of a curve $L(k)$ changes depending on the scale k used as unit of measurement. Our FD measure is based on the Higuchi algorithm, implemented in function *featureExtraction2* (Figure 7). The Higuchi's standard approach calculates FD of time series in the time domain, and is based on the $log[L(k)]$ vs $log(k)$ curve, which is computed as follow [8]:

- For each sample *i* of the EEG epoch $\boldsymbol{x} = \{x(1), x(2), \ldots, x(N)\}$ of length *N*, the absolute differences between values $x(i)$ and $x(i - k)$, i.e., the samples at distance *k,* are computed, considering $k = 1, \ldots, k_{max}$;
- Each absolute difference is multiplied by a normalization coefficient that considers the different numbers of samples available for each value of *k*. The computation of this coefficient is based on the starting point $m = 1, \ldots, k$ and on the total number *N* of samples of an epoch;
- $L_m(k)$ is computed as:

$$L_m(k) = \frac{1}{k} \cdot \left[\sum_{i=1}^{q} |x(m + i \cdot k) - x(m + (i-1) \cdot k)| \right] \cdot \frac{N-1}{q \cdot k}$$

  where $q = int[(N - m)/k]$;
- $L(k)$ is computed by summing the obtained values and dividing by k;
- The $log[L(k)]$ vs $log(k)$ curve, referred to in the following as l_k, is finally derived.

By definition, if $L(k)$ is proportional to k^{-D} (i.e., $log(k)$ and $log[L(k)]$) have a linear relationship) for $k = 1, \ldots, k_{lin}$, then the curve is fractal with dimension D. Thus, k_{lin} is the maximum k for which $L(k)$ is proportional to k^{-D} and D is estimated by ordinary least squares as the linear coefficient of the regression line of the l_k curve for $k = 1, \ldots, k_{lin}$.

Particularly, we extracted epochs of 4 s from each signal, with an overlapping of 2 s. The linear region was defined by imposing a k_{lin} equal to 6, while k_{max} was chosen equal to 35 according to [5] and considering the different sampling frequency. Indeed, the actual sampling frequency is 250 Hz while in [5] it was 128 Hz, so k_{max} was increased proportionally from 18 to 35.

We decided to consider the median of the Higuchi's measures to obtain a single value for each channel, as suggested by Rubega et al. in [7].

```
%% PRE
H = zeros(1,Nch);
for i = 1:Nch
    count = 1;

    for k = 1+overlap:overlap:Ns-overlap
        segments(count,:) = data_pre_pp(k-overlap:k+overlap-1,i);
        count = count + 1;
    end

    [Higuchi, output_lnk, output_lnLk] = featuresExtraction2(segments, klin, kmax);
    H_all(i, :) = Higuchi;
    H(i) = median(Higuchi);
    if i == 30
        figure
        plot(output_lnk(1,:), median(output_lnLk), 'r', 'LineWidth', 1)
        xlabel('log(k)')
        ylabel('log(L_k)')
        title('log(L_k) vs log(k) (Cz)')
        hold on

        [f,xi] = ksdensity(Higuchi);

    end
end
```

Figure 7: Matlab code used for the computation of Higuchi's FD measures for the pre-signal. A similar code was implemented for the post-signal.

2.5 Evaluation of changes before and after EAG

To assess changes in linear and nonlinear metrics before and after EAG, we adopted both a qualitative (visual inspection) and quantitative (statistical test) approach. We decided to apply t-test if data were normally distributed, and Wilcoxon rank-sum test otherwise (alpha = 0.05).

3. Results and discussion

No significant differences were found in the relative power in theta, delta, and alpha bands, while the statistical tests revealed a significant decrease in the relative power in beta band (p-value = 0.0012). (Figure 8)

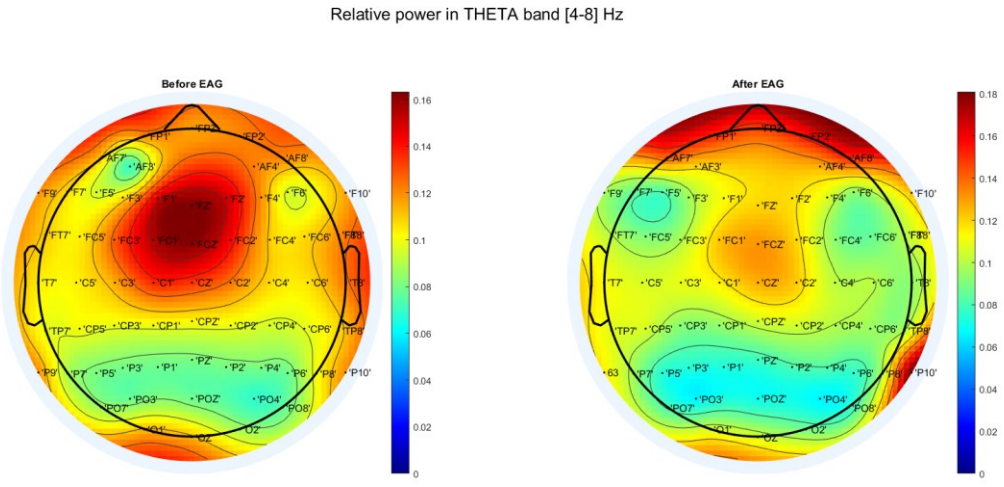

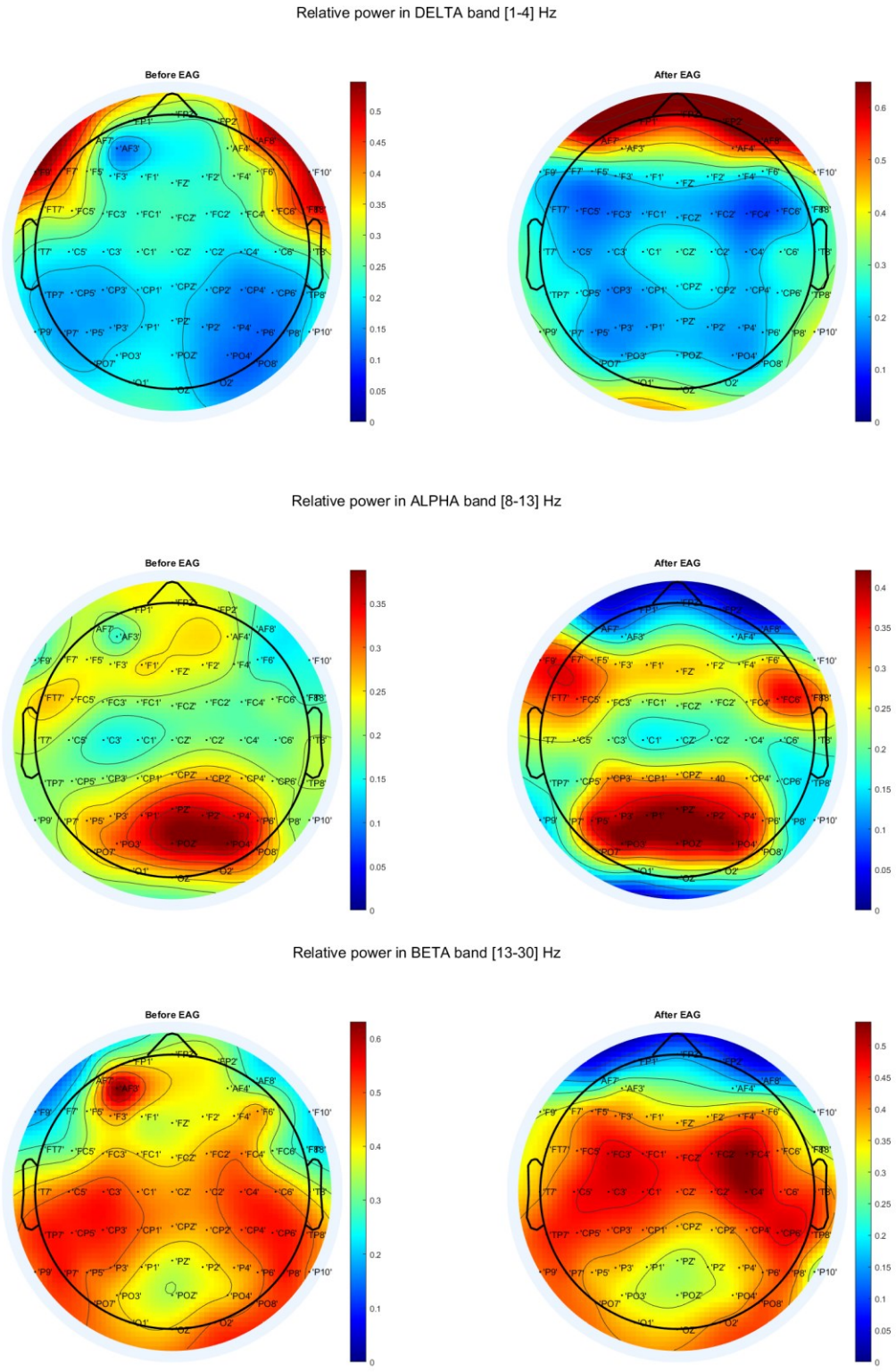

Figure 8: Relative power distribution in the canonical frequency EEG bands.

No statistical differences were found taking into account Higuchi's FD median values for each channel. Considering that we are analysing a healthy subject, this result could be consistent with the patient's condition. (Figure 9)
In contrast, we found statistical differences analysing each channel singularly as reported in Figure 10. Focusing on Cz channel, the one in which we expected to find feet movement related activity, a significant increase in Higuchi's FD values was found, highlighting an increase in signal complexity after EAG. (Figure 11)

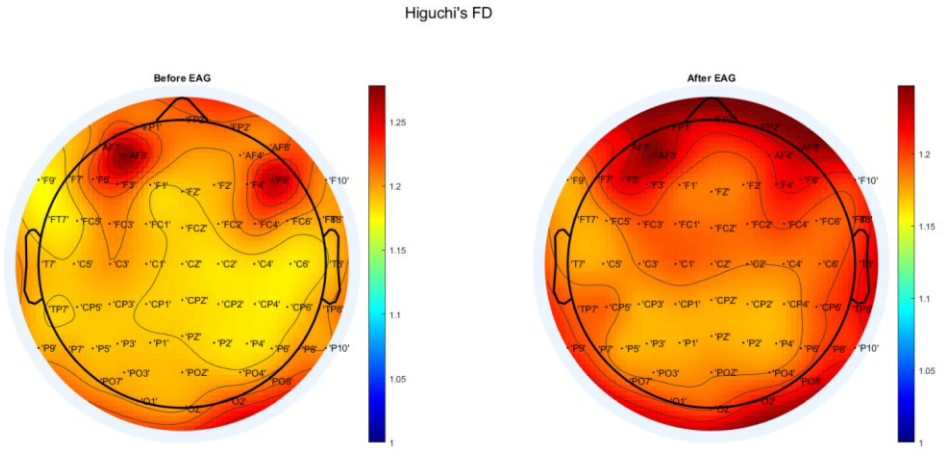

Figure 9: Higuchi's FD median values distribution.

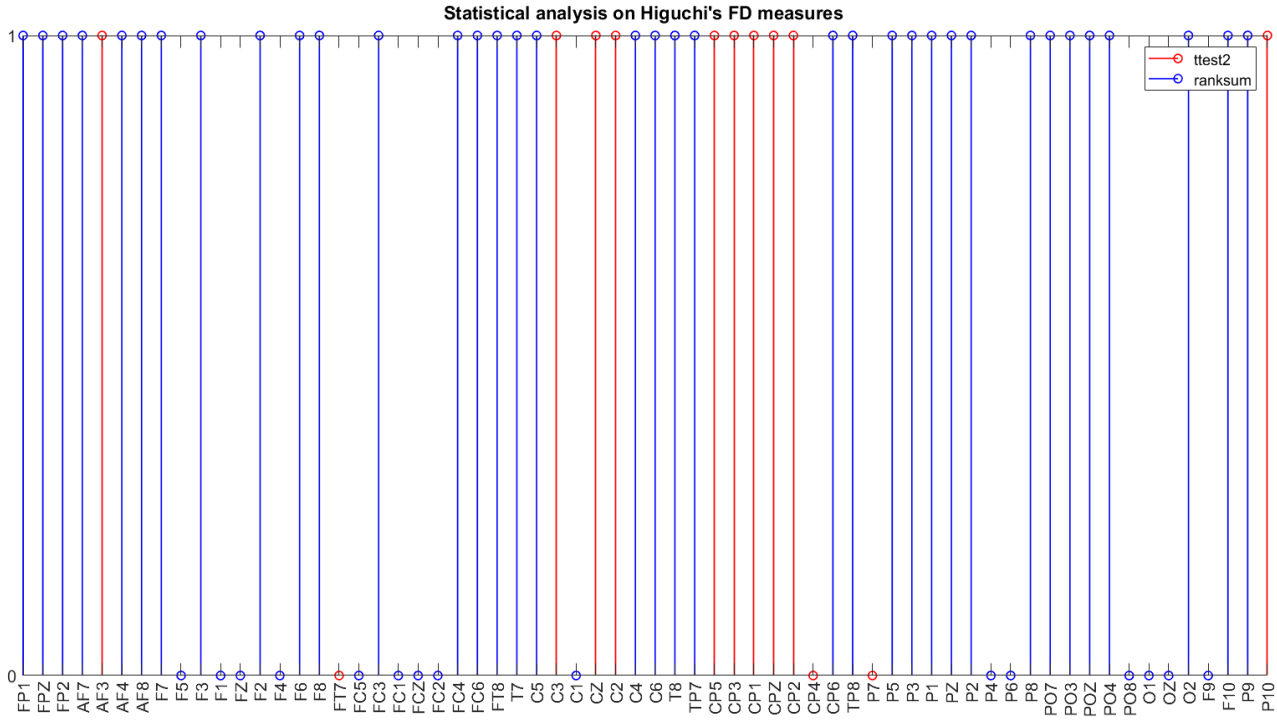

Figure 10: Results of statistical tests on Higuchi's FD measures.

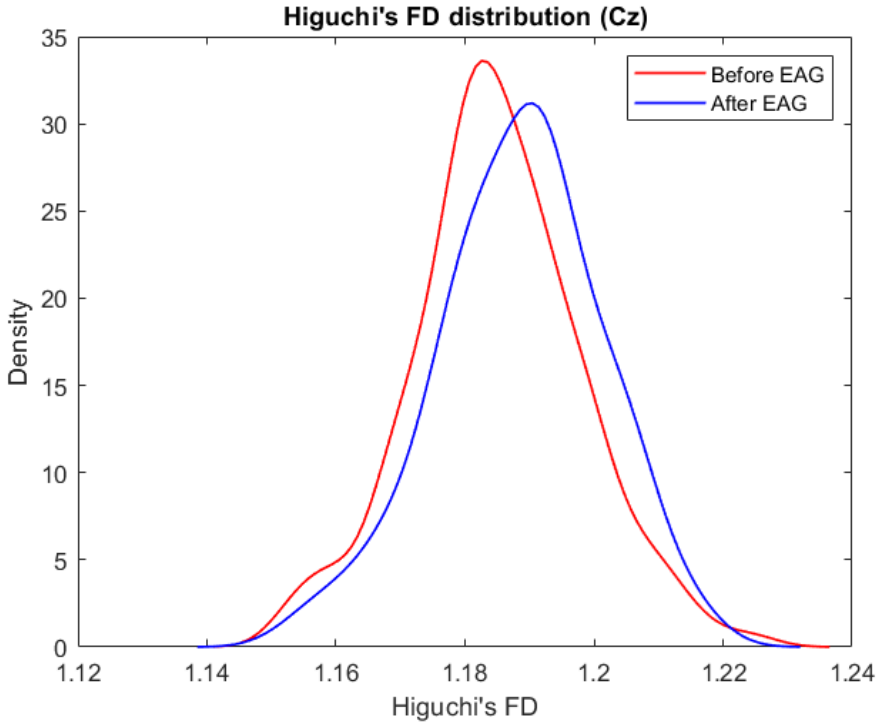

Figure 11: Cz channel distribution of Higuchi's FD measures before and after EAG.

4. Conclusion

In this work we investigated EEG variations induced by a single session of EAG, through both linear and nonlinear approaches. Our results show no overall differences for the studied metrics (relative power spectrum and Higuchi's FD), even though statistical differences at single channel level for Higuchi's FD measures were found. Since literature suggests Cz channel to be more likely involved in processing information related to feet movement, we focused our attention on it, as one of the most relevant for our EAG task. We highlighted a significant increase in Higuchi's FD, suggesting an incrementation in signal complexity after an EAG session. Probably, the application of the explored methods on a diseased subject EEG data could reveal more significant changes in brain activity to assess the impact of EAG training.

Bibliography

[1] Jang TG, Choi SH, Yu SH, Kim DH, Han IH, Nam KH. Exoskeleton-assisted Gait Training in Spinal Disease With Gait Disturbance. *Korean J Neurotrauma*. 2022;18(2):316-323. Published 2022 May 2. doi:10.13004/kjnt.2022.18.e25

[2] Al-Quraishi MS, Elamvazuthi I, Daud SA, Parasuraman S, Borboni A. EEG-Based Control for Upper and Lower Limb Exoskeletons and Prostheses: A Systematic Review. Sensors (Basel). 2018 Oct 7;18(10):3342. doi: 10.3390/s18103342. PMID: 30301238; PMCID: PMC6211123.

[3] Zappasodi F, Olejarczyk E, Marzetti L, et al. Fractal dimension of EEG activity senses neuronal impairment in acute stroke. Plos one. 2014 ;9(6):e100199. DOI: 10.1371/journal.pone.0100199. PMID: 24967904; PMCID: PMC4072666.

[4] Accardo A, Affinito M, Carrozzi M, Bouquet F. Use of the fractal dimension for the analysis of electroencephalographic time series. Biol Cybern. 1997 Nov;77(5):339-50. doi: 10.1007/s004220050394. PMID: 9418215.

[5] F. Finotello, F. Scarpa, M. Zanon, EEG signal features extraction based on fractal dimension, in: Conf Proc IEEE Eng Med Biol Soc, Milan, 2015.

[6] Rubega M, Scarpa F, Teodori D, Sejling AS, Frandsen CS, Sparacino G. Detection of Hypoglycemia Using Measures of EEG Complexity in Type 1 Diabetes Patients. Entropy (Basel). 2020 Jan 9;22(1):81. doi: 10.3390/e22010081. PMID: 33285854; PMCID: PMC7516516.

[7] Rubega, M.; Formaggio, E.; Molteni, F.; Guanziroli, E.; Di Marco, R.; Baracchini, C.; Ermani, M.; Ward, N.S.; Masiero, S.; Del Felice, A. EEG Fractal Analysis Reflects Brain Impairment after Stroke. *Entropy* **2021**, *23*, 592. https://doi.org/10.3390/e23050592

[8] Fabio Scarpa, Maria Rubega, Mattia Zanon, Francesca Finotello, Anne-Sophie Sejling, Giovanni Sparacino, Hypoglycemia-induced EEG complexity changes in Type 1 diabetes assessed by fractal analysis algorithm. ELSEVIER, Biomedical Signal Processing and Control 38 (2017) 168–173, https://doi.org/10.1016/j.bspc.2017.06.004